

Linear Heterotrinnuclear Complexes Derived from an Alkyl Platinum(II) Twelve-Membered Macrocycle[†]

Hai-Bin Song,[†] Zheng-Zhi Zhang,[‡] Zheng Hui,[§] Chi-Ming Che,[§] and Thomas C. W. Mak^{*†}

Department of Chemistry, The Chinese University of Hong Kong, Shatin, New Territories, Hong Kong SAR, P. R. China, State Key Laboratory of Elemento-Organic Chemistry, Nankai University, Tianjin, P. R. China, and Department of Chemistry and the HKU-CAS Joint Laboratory on New Materials, The University of Hong Kong, Pokfulam Road, Hong Kong SAR, P. R. China

Received December 18, 2001

The *P,N,P*-tridentate ligand 2,6-bis(diphenylphosphino)pyridine, L, was employed to generate a twelve-membered metallomacrocyclic host species *cis*-Pt₂Me₄(μ -L)₂ that encapsulates Tl(I) and Cu(I) guest ions. The ligand was also used to synthesize another two linear heterotrinnuclear complexes, [Me₂Pt(μ -L)₂Ag₂(MeCN)₂](BF₄)₂·MeCN and [(CO)₃Fe(μ -L)₂Ag₂(Et₂O)](ClO₄)₂, both containing a metal–metal dative bond (Pt→Ag and Fe→Ag, respectively) and stabilized by the d¹⁰–d¹⁰ argentophilic interaction.

Introduction

Metallomacrocyclic complexes have developed rapidly in recent years because of their encapsulating capability, photophysical properties, and potential applications in catalysis, sensing, molecular electronics, and facilitated small molecule transport.¹ A variety of strategies have been employed.² The approach which utilized multidentate hemilabile ligands, typically phosphinopyridine and phosphinoalkyl ether, was mostly used. The different coordination ability of hard and soft donor atoms and variable spacer lengths between the donor atoms enable the ligand to form various metallomacrocycles which may encapsulate metal ions and small molecules. Balch and co-workers found that an electron-rich metal atom such as Rh or Ir (usually in low oxidation state) acted as a soft base in this type of reaction.³ Recently, the bonding interaction between closed-shell metal atoms or ions is gaining increasing attention, and while there exist numerous examples of fluorophenyl and cyanate platinum(II) centers aggregating with s² ions such as Tl(I) or Pb(II) and d¹⁰ ions such as Au(I) or Ag(I),⁴ there are few

reports of similar association in the case of alkyl platinum(II) complexes.

The past decade has witnessed a phenomenal growth in the study of linear metal arrays (metal wires) in view of their unique structural features and special properties.⁵ In general, the bonding in such metallic chains may involve single or multiple covalent bonding^{5a–e} and/or donor–acceptor

* To whom correspondence should be addressed. E-mail: tcwmak@cuhk.edu.hk. Fax: (852) 2603 5057.

[†] Dedicated to the memory of Dr. Richard K. McMullan (1929–2002).

[‡] The Chinese University of Hong Kong.

[§] Nankai University.

[§] The University of Hong Kong.

(1) Lehn, J.-M. *Supramolecular chemistry*; VCH: New York, 1995.

(2) Swiegers, G. F.; Malefetse, T. J. *Chem. Rev.* **2000**, *100*, 3483.

(3) Balch, A. L.; Rowley, S. P. *J. Am. Chem. Soc.* **1990**, *112*, 6139. (b) Balch, A. L. *Prog. Inorg. Chem.* **1993**, *41*, 239.

(4) Catalano, V. J.; Benett, B. L.; Yson, R. L.; Noll, B. C. *J. Am. Chem. Soc.* **2000**, *122*, 10056. (b) Catalano, V. J.; Benett, B. L.; Noll, B. C. *Chem. Commun.* **2000**, 1413. (c) Uson, R.; Fornies, J.; Tomas, M.; Garde, R.; Merino, R. I. *Inorg. Chem.* **1997**, *36*, 1383. (d) Ara, I.; Berenguer, J. R.; Fornies, J.; Gomez, J.; Lalinde, E.; Merino, R. I. *Inorg. Chem.* **1997**, *36*, 6461. (e) Uson, R.; Fornies, J.; Tomas, M.; Garde, R. *J. Am. Chem. Soc.* **1995**, *117*, 1837. (f) Catalano, V. J.; Benett, B. L.; Muratidis, S.; Noll, B. C. *J. Am. Chem. Soc.* **2001**, *123*, 173. (g) Uson, R.; Fornies, J.; Falvello, L. R.; Uson, M. A.; Uson, I. *Inorg. Chem.* **1992**, *31*, 3697.

(5) Finnis, G. M. E.; Canadell, Campana, C.; Dunbar, K. R. *Angew. Chem., Int. Ed. Engl.* **1996**, *35*, 2772. (b) Chen, Y.-H.; Lee, C.-C.; Wang, C.-C.; Lee, G.-H.; Lai, S.-Y.; Li, F.-Y.; Mou, C.-Y.; Peng, S.-M. *Chem. Commun.* **1999**, 1667. (c) Sakai, K.; Tanaka, Y.; Tsuchiya, Y.; Hirata, K.; Tsubomura, T.; Iijima, S.; Bhattacharjee, A. *J. Am. Chem. Soc.* **1998**, *120*, 8366. (d) Lai, S.-Y.; Lin, T.-W.; Chen, Y.-H.; Wang, C.-C.; Lee, G.-H.; Yang, M.-H.; Leung, M.-K.; Peng, S.-M. *J. Am. Chem. Soc.* **1998**, *121*, 250 and references therein. (e) Clerac, R.; Cotton, F. A.; Dunbar, K. R.; Lu, T. B.; Murillo, C. A.; Wang, X. P. *J. Am. Chem. Soc.* **2000**, *122*, 2272 and references therein. (f) Balch, A. L.; Catalano, V. J.; Olmstead, M. M. *J. Am. Chem. Soc.* **1990**, *112*, 2010 and references therein. (g) Uang, R.-H.; Chan, C.-K.; Peng, S.-M.; Che, C.-M. *J. Chem. Soc., Chem. Commun.* **1994**, 2561. (h) Catalano, V. J.; Malwitz, M. A.; Noll, B. C. *Chem. Commun.* **2001**, 581 and references therein. (i) Tsai, M.-S.; Peng, S.-M. *J. Chem. Soc., Chem. Commun.* **1991**, 514. (j) Li, D.; Che, C.-M.; Peng, S.-M.; Liu, S.-T.; Zhou, Z.-Z.; Mak, T. C. W. *J. Chem. Soc., Chem. Commun.* **1991**, 1615. (k) Xiao, H.; Weng, Y.-X.; Wong, W.-T.; Mak, T. C. W.; Che, C.-M. *J. Chem. Soc., Dalton Trans.* **1997**, 221.

bonding^{5f–h} between adjacent atoms. More recently, another type of noncovalent metal–metal (metallophilic) interaction, namely the d^{10} – d^{10} contact, has been shown to occur in such systems.^{5i–k} The aurophilic interaction, which is well-established for many gold(I)–phosphine complexes,^{6a} has been attributed to a combination of correlation and relativistic effects.^{6b} More recently, experimental evidence has been gathered to support the significance of analogous argentophilic^{6c} and cuprophilic^{6d} interactions in a variety of silver(I) and copper(I) complexes. To our knowledge, there is as yet no report of a linear trinuclear system containing both the metal–metal donor–acceptor bond and d^{10} – d^{10} contact.

2,6-Bis(diphenylphosphino)pyridine, L, is a *P,N,P*-tridentate ligand of which four coordination modes A–D are known (Figure 1).⁷ To date, there are only two examples of symmetrical heterotrinnuclear $M-M'-M$ complexes, namely $[\text{Ir}_2\text{CuCl}_2(\text{CO})_2(\mu\text{-L})_2(\text{MeCN})]\text{ClO}_4$ ^{7m} and $[\{\text{Fe}(\text{CO})_4\}_2\text{Ag}(\mu\text{-L})]\text{ClO}_4$ ⁷ⁿ that adopt symmetrical mode D in which the phosphorus atoms of the bridging ligand L each coordinate to the same type of metal atom. The unsymmetrical coordination mode E, in which (i) the phosphorus atoms of L coordinate to different types of metal atoms, and (ii) consecutive pairs of unlike and like metal atoms are connected by donor–acceptor bonding and d^{10} – d^{10} interaction, respectively, is quite rare, as only three examples of Pt–Pt–M (M = Rh, Ir, Pd) systems bridged by bis(diphenylphosphinomethyl)-phenylphosphine have been reported.⁸

In the present work, we used bridging ligand L to generate a twelve-membered alkyl platinum(II) metallomacrocyclic whose encapsulation of Tl(I) and Cu(I) ions was investigated, as well as two linear heterotrinnuclear systems featuring both metal–metal donor–acceptor bonding and d^{10} – d^{10} argentophilic interaction.

Experimental Section

Synthesis of Compounds. Unless otherwise stated, all reactions were performed under a nitrogen atmosphere using standard Schlenk

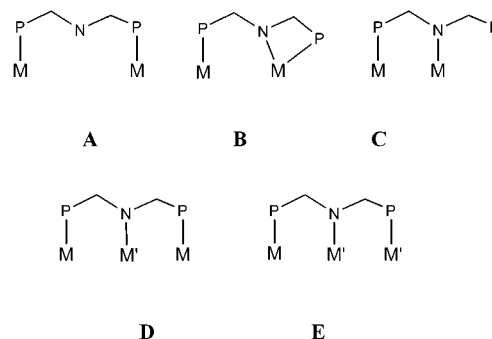


Figure 1. Coordination modes of 2,6-bis(diphenylphosphino)pyridine, L.

techniques. The solvents were purified by standard methods. The ligand (Ph_2P)₂py (L) was prepared by the published procedure.^{7a}

CAUTION. While none of the perchlorate complexes has proved to be shock sensitive, proper care should nevertheless always be taken to work with them.

[Me₂Pt(μ-L)]₂, 1. A 0.13 g (0.4 mmol) portion of $\text{PtMe}_2(\text{cod})$ and 0.18 g (0.4 mmol) of L was mixed in 10 mL of CH_2Cl_2 , and the solution was stirred for 20 min. Then, the solution was concentrated in vacuo to ~2 mL, and diffusion of hexane into it gave a white powder of **1** in 80% yield. (Anal. Found: C, 55.06; H, 4.68; N, 2.23. Calcd for $\text{C}_{62}\text{H}_{58}\text{N}_2\text{P}_4\text{Pt}_2$: C, 55.36; H 4.35; N, 2.08.) ³¹P{¹H}NMR: δ 29.1 (sd) with $^1J(^{195}\text{Pt}, ^{31}\text{P}) = 1883$ Hz.

[[Me₂Pt(μ-L)]₂Tl]ClO₄, 2. A 0.03 g (0.1 mmol) portion of **1** was added to 0.031 g (0.1 mmol) of TlClO_4 suspended in 5 mL of CH_2Cl_2 . The mixture was stirred for 2 h, and the solution was concentrated to 2 mL and then filtered. Slow diffusion of ethyl ether into the filtrate gave a yellow powder of **2** in 60% yield. Single crystals of **2**·1.5THF were obtained from slow evaporation of a THF solution. (Anal. Found: C, 45.32; H, 3.70; N, 1.82. Calcd for $\text{C}_{62}\text{H}_{58}\text{ClN}_2\text{O}_4\text{P}_4\text{Pt}_2\text{Tl}$: C, 45.16; H, 3.54; N, 1.70.) ³¹P{¹H}NMR: δ 32.7 (sd) with $^1J(^{195}\text{Pt}, ^{31}\text{P}) = 1688$ Hz.

[[Me₂Pt(μ-L)]₂Cu]ClO₄, 3. A 0.02 g (0.06 mmol) portion of $[\text{Cu}(\text{MeCN})_4]\text{ClO}_4$ was added to a solution of 0.1 g (0.06 mmol) of **2** in 5 mL of CH_2Cl_2 . The mixture was stirred, and the color changed from yellow to orange. After stirring for 20 min, the solution was concentrated to 2 mL and then filtered. Slow diffusion of ethyl ether into the filtrate gave prismatic red-orange crystals of **3**·0.5H₂O in 95% yield. (Anal. Found: C, 49.32; H, 3.70; N, 1.80. Calcd for $\text{C}_{62}\text{H}_{58}\text{ClN}_2\text{O}_4\text{P}_4\text{Pt}_2\text{Cu}$: C, 49.38; H, 3.88; N, 1.86.) ³¹P{¹H}NMR: δ 33.9(sd) with $^1J(^{195}\text{Pt}, ^{31}\text{P}) = 1586$ Hz.

[[Me₂Pt(μ-L)]₂Cu]BF₄, 4. A 0.024 g (0.076 mmol) portion of $[\text{Cu}(\text{MeCN})_4]\text{BF}_4$ was added to a solution of 0.1 g (0.076 mmol) of **1** in 5 mL of CH_2Cl_2 . The mixture was stirred, and the color changed to orange. After stirring for 20 min, the solution was concentrated to 2 mL and then filtered. Slow diffusion of ethyl ether into the filtrate gave prismatic red-orange crystals **4**·0.5H₂O in 80% yield. (Anal. Found: C, 49.79; H, 3.91; N, 1.87. Calcd for $\text{C}_{62}\text{H}_{58}\text{BF}_4\text{N}_2\text{P}_4\text{Pt}_2\text{Cu}$: C, 49.64, H, 3.74, N, 1.82.) ³¹P{¹H}NMR: δ 33.9(sd) with $^1J(^{195}\text{Pt}, ^{31}\text{P}) = 1586$ Hz.

[Me₂Pt(μ-L)₂Ag₂(MeCN)₂](BF₄)₂, 5. A 0.1 g (0.11 mmol) portion of $[\text{Ag}_2(\text{MeCN})_2(\mu\text{-L})](\text{BF}_4)_2$ ^{7c–d} 0.05 g (0.11 mmol) of L, and 0.35 g $\text{PtMe}_2(\text{cod})$ were mixed in 10 mL $\text{CH}_2\text{Cl}_2/\text{MeCN}$ (1:1), and the solution was stirred for 20 min. Then, the solution was concentrated in vacuo to ~2 mL, and slow diffusion of diethyl ether into it gave pale yellow crystals of **5**·MeCN in 95% yield. (Anal. Found: C, 44.77; H, 3.68; N, 3.23. Calcd for $\text{C}_{64}\text{H}_{58}\text{B}_2\text{N}_4\text{F}_8\text{P}_4\text{Ag}_2\text{Pt}$: C, 48.24; H, 3.79; N, 3.51.) ³¹P{¹H}NMR: 34.8(sd) with $^1J(^{195}\text{Pt}, ^{31}\text{P}) = 1547$ Hz, 25.1(dd) with $^1J(^{109}\text{Ag}, ^{31}\text{P}) = 529$ Hz and $^1J(^{107}\text{Ag}, ^{31}\text{P}) = 457$ Hz.

- (6) Schmidbaur, H. *Chem. Soc. Rev.* **1995**, *24*, 391. (b) Pyykkö, P. *Chem. Rev.* **1997**, *97*, 597. (c) Wang, Q.-M.; Mak, T. C. W. *J. Am. Chem. Soc.* **2001**, *123*, 7600 and references therein. (d) Che, C.-M.; Mao, Z.; Miskowski, V. M.; Tse, M.-C.; Chan, C.-K.; Cheung, K.-K.; Phillips, D. L.; Leung, K. H. *Angew. Chem., Int. Ed.* **2000**, *39*, 4084. (7) Newkome, G. R.; Hager, D. C. *J. Org. Chem.* **1978**, *43*, 947. (b) Wood, F.; Olmstead, M. M.; Balch, A. L. *J. Am. Chem. Soc.* **1983**, *105*, 6332. (c) Wood, F. E.; Hvorslef, J.; Hope, H.; Balch, A. L. *Inorg. Chem.* **1984**, *23*, 4309. (d) Wood, F. E.; Hvorslef, J.; Balch, A. L. *J. Am. Chem. Soc.* **1983**, *105*, 6986. (e) Shieh, S.-J.; Li, D.; Peng, S.-M.; Che, C.-M. *J. Chem. Soc., Dalton Trans.* **1993**, 195. (f) Shieh, S.-J.; Hong, X.; Peng, S.-M.; Che, C.-M. *J. Chem. Soc., Dalton Trans.* **1993**, 3067. (g) Field, J. S.; Haines, R. J.; Warwick, B.; Zulu, M. M. *Polyhedron* **1996**, *15*, 3471. (h) Kuang, S.-M.; Zhang, L.-M.; Zhang, Z.-Z.; Wu, B.-M.; Mak, T. C. W. *Inorg. Chim. Acta* **1999**, *284*, 278. (i) Kuang, S.-M.; Zhang, Z.-Z.; Wang, Q.-G.; Mak, T. C. W. *J. Chem. Soc., Chem. Commun.* **1998**, 581. (j) Balch, A. L.; Fossett, L. A.; Olmstead, M. M. *Inorg. Chem.* **1986**, *25*, 4526. (k) Cotton, F. A.; Dikarev, E. V.; Jordan, G. T., IV; Murillo, C. A.; Petrukhina, M. A. *Inorg. Chem.* **1998**, *37*, 4611. (l) Balch, A. L.; Hope, H.; Wood, F. E. *J. Am. Chem. Soc.* **1985**, *107*, 6936. (m) Kuang, S.-M.; Zhang, Z.-Z.; Wang, Q.-G.; Mak, T. C. W. *Polyhedron* **1998**, *18*, 493. (n) Song, H.-B.; Zhang, Z.-Z.; Mak, T. C. W. *Inorg. Chem.* **2001**, *40*, 5928 and references therein. (8) Tanase, T.; Toda, H.; Kobayashi, K.; Yamamoto, Y. *Organometallics* **1996**, *15*, 5272. (b) Tanase, T.; Ukaji, H.; Takahata, H.; Toda, H.; Igoshi, T.; Yamamoto, Y. *Organometallics* **1998**, *17*, 196.

Table 1. X-ray Crystallographic Data and Refinement Parameters of the Complexes

complex	2·1.5THF	3·0.5H ₂ O	4·0.5H ₂ O	5·MeCN	6
formula	C ₇₀ H ₆₈ ClN ₂ O ₇ - P ₄ Pt ₂ Tl	C ₆₂ H ₅₉ ClCuN ₂ - O _{4.5} P ₄ Pt ₂	C ₆₂ H ₅₉ BcuF ₄ N ₂ - O _{0.5} P ₄ Pt ₂	C ₆₆ H ₆₁ Ag ₂ B ₂ F ₈ - N ₅ P ₄ Pt	C ₆₅ H ₅₆ Ag ₂ Cl ₂ Fe- N ₂ O ₁₂ P ₄
mol wt	1803.14	1517.16	1504.52	1632.53	1523.49
cryst syst	triclinic	triclinic	triclinic	triclinic	triclinic
space group	<i>P</i> $\bar{1}$ (No. 2)	<i>P</i> $\bar{1}$ (No. 2)	<i>P</i> $\bar{1}$ (No. 2)	<i>P</i> $\bar{1}$ (No. 2)	<i>P</i> $\bar{1}$ (No. 2)
cryst size/mm ³	0.46 × 0.38 × 0.10	0.32 × 0.20 × 0.18	0.50 × 0.20 × 0.18	0.44 × 0.24 × 0.22	0.42 × 0.18 × 0.16
<i>a</i> /Å	13.006(2)	11.244(1)	11.3173(4)	13.0418(8)	14.235(1)
<i>b</i> /Å	14.218(3)	13.793(2)	13.7285(5)	16.617(1)	15.935(2)
<i>c</i> /Å	21.486(4)	22.030(2)	22.1019(8)	17.033(1)	16.781(2)
α /°	71.709(3)	96.824(2)	96.287(1)	88.402(1)	72.840(2)
β /°	81.242(4)	102.047(2)	99.722(1)	86.601(1)	68.326(2)
γ /°	64.587(4)	111.745(2)	111.279(1)	72.470(1)	68.607(2)
<i>U</i> /Å ³	3406.5(10)	3030.3(6)	3098.88(19)	3513.4(4)	3235.5(5)
<i>Z</i>	2	2	2	2	2
<i>D</i> _c /g cm ⁻³	1.758	1.663	1.612	1.543	1.564
<i>F</i> (000)	1744	1486	1470	1612	1540
μ (Mo K α)/mm ⁻¹	6.642	5.150	4.998	2.691	1.064
total reflns	18376	20759	21254	23977	22716
no. unique reflns (<i>R</i> _{int})	11951 (0.071) ^b	14377 (0.046)	14688 (0.043)	16662 (0.034)	15280 (0.028)
no. obsd reflns	6799	7407	7949	9380	8484
no. variables	746	709	681	739	820
<i>P</i>					
GOF	0.980	0.871	0.877	0.913	0.899
R1, wR2	0.0679, 0.1627	0.0521, 0.1124	0.0523, 0.1135	0.0504, 0.1233	0.0454, 0.0916
[<i>I</i> > 2 σ (<i>I</i>)] ^a					
R1, wR2 (all data)	0.1295, 0.1881	0.1158, 0.1383	0.1073, 0.1289	0.1040, 0.1400	0.0925, 0.1079

^a R1 = $\sum(|F_o| - |F_c|)/\sum|F_o|$, wR2 = $\{\sum(|F_o| - |F_c|)^2/\sum|F_o|^2\}^{1/2}$. ^b DIFABS absorption correction was applied.

[(CO)₃Fe(μ -L)₂Ag₂(Et₂O)](ClO₄)₂, **6**. A 1.1 g (2.5 mmol) portion of L in CH₂Cl₂ (20 mL) was added to an ethanol solution (20 mL) of H₂Fe(CO)₄ (1 mmol) and H₂SO₄ (1.5 mmol) at ambient temperature. The solution was stirred for 3 h, during which a copious amount of yellow precipitate appeared. After the reaction was completed, the solution was concentrated in vacuo to ~20 mL, and the solid was filtered off and washed successively with water and ethanol and several times with diethyl ether. The solid was then redissolved in CH₂Cl₂ (20 mL), and 0.4 g AgClO₄ was added to the solution with stirring. After stirring for 30 min, the solution was concentrated to 10 mL and then filtered. Slow diffusion of ethyl ether into the filtrate gave yellow crystals of **6** in 65% yield. (Anal. Found: C, 51.04; H, 3.72; N, 1.80. Calcd for C₆₅H₅₆Ag₂Cl₂FeN₂O₁₂P₄: C, 51.24; H, 3.71; N, 1.84.) IR(ν CO): 1991 s, 1931 s, 1896 cm⁻¹. ³¹P{¹H}NMR 87.2 (d) with *J*(Ag, P) = 12 Hz, 27.8 (dd) with ¹*J*(¹⁰⁹Ag, ³¹P) = 536 Hz and ¹*J*(¹⁰⁷Ag, ³¹P) = 463 Hz.

X-ray Crystallography. For each of **2**·1.5THF, **3**·0.5H₂O, **4**·0.5H₂O, **5**·MeCN, and **6**, a selected single crystal was mounted on a Bruker SMART 1000 CCD diffractometer operating at 50 kV and 30 mA using Mo K α radiation (λ = 0.71073 Å). Data collection at 293 K and reduction were performed using the SMART and SAINT software,⁹ with frames of 0.3° oscillation in the θ range 1.5° < θ < 28° (for **2**·1.5THF, 1.5° < θ < 25°). An empirical absorption correction (SADABS) was applied to the raw intensities.¹⁰ DIFABS absorption correction was also applied to **2**·1.5THF.¹¹ The crystal structures were determined by direct methods and refined by full-matrix least squares using the SHELXTL-PC program package.¹² Non-hydrogen atoms were subjected to aniso-

tropic refinement. All hydrogen atoms were generated geometrically (C–H bond lengths fixed at 0.96 Å), assigned appropriate isotropic thermal parameters, and included in structure factor calculations in the final stage of *F*² refinement. A summary of the crystal data is given in Table 1. Selected bond lengths and bond angles are listed in Table 2 (compounds **2**–**4**) and Table 4 (compounds **5** and **6**). Further details are given in the Supporting Information.

Spectroscopic Measurements. Infrared spectra were recorded on a Nicolet impact 420 spectrometer using KBr disks. ³¹P{¹H} NMR spectra were recorded on an JEOL EX270 spectrometer at 109.25 MHz using H₃PO₄ as the external standard and CDCl₃ as solvent. Solutions for excitation or emission measurements were degassed by at least four freeze–pump–thaw cycles. Absorption spectra were recorded at ambient temperature with a HP8453 UV–vis spectrophotometer. Emission and excitation spectra were obtained on a SPEX Fluorolog-2 emission spectrophotometer adapted to a right-angle configuration. Filters of suitable band-pass were used to cut off the second harmonic of the monochromatic excitation light source and stray light. Emission lifetimes of solution samples were performed with a Quanta Ray DCR-3 Nd:YAG laser with pulse-width of 8 ns and excitation wavelength of 355 nm (third harmonic). Emission signals were collected at right angles to the excitation pulse by a Hamamatsu R928 photomultiplier tube and recorded on a Tektronix model 2430 digital oscilloscope.

Result and Discussion

Synthetic Studies and Structures of 2–6. The reaction of L with Me₂Pt(cod) (cod = 1,5-cyclooctadiene) in CH₂Cl₂ in molar ratio 1:1 gave **1** (80% yield) as a white powder. The elemental analysis showed that **1** has a formula C₃₁H₂₉–

(9) SMART 5.0 and SAINT 4.0 for Windows NT: Area Detector Control and Integration Software; Bruker Analytical X-ray Systems, Inc.: Madison, WI, 1998.

(10) Sheldrick, G. M. SADABS: Program for Empirical Absorption Correction of Area Detector Data; University of Göttingen: Germany, 1996.

(11) Walker N.; Stuart, D. *Acta Crystallogr., Sect. A* **1983**, *39*, 158.

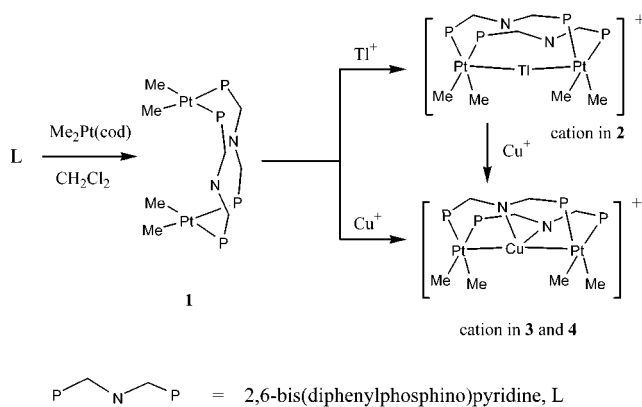
(12) Sheldrick, G. M. SHELXTL 5.10 for Windows NT: Structure Determination Software Programs; Bruker Analytical X-ray Systems, Inc.: Madison, WI, 1997.

Table 2. Selected Bond Distances (Å) and Angles (deg) for Complexes 2, 3, and 4

	2		3	4
Pt(1)–C(1)	2.057(12)	Pt(1)–C(1)	2.092(9)	2.113(8)
Pt(1)–C(2)	2.128(9)	Pt(1)–C(2)	2.08(1)	2.11(1)
Pt(1)–P(1)	2.352(3)	Pt(1)–P(1)	2.300(3)	2.309(2)
Pt(1)–P(3)	2.327(2)	Pt(1)–P(3)	2.326(3)	2.324(2)
Pt(1)–Tl(1)	2.7961(7)	Pt(1)–Cu(1)	2.591(1)	2.595(1)
Pt(2)–C(4)	2.063(9)	Pt(2)–C(3)	2.094(9)	2.07(1)
Pt(2)–C(3)	2.097(10)	Pt(2)–C(4)	2.116(9)	2.103(8)
Pt(2)–P(2)	2.306(3)	Pt(2)–P(4)	2.297(3)	2.306(2)
Pt(2)–P(4)	2.322(2)	Pt(2)–P(2)	2.319(2)	2.322(2)
Pt(2)–Tl(1)	2.8090(7)	Pt(2)–Cu(1)	2.622(1)	2.620(1)
C(1)–Pt(1)–C(2)	82.3(4)	Cu(1)–N(1)	1.974(7)	1.963(7)
C(1)–Pt(1)–P(3)	88.6(3)	Cu(1)–N(2)	1.982(8)	1.983(6)
C(2)–Pt(1)–P(3)	170.7(3)	C(1)–Pt(1)–C(2)	83.9(4)	81.7(4)
C(1)–Pt(1)–P(1)	166.9(2)	C(1)–Pt(1)–P(1)	175.6(3)	175.0(3)
C(2)–Pt(1)–P(1)	87.7(3)	C(2)–Pt(1)–P(1)	92.0(3)	93.3(3)
P(3)–Pt(1)–P(1)	101.61(9)	C(1)–Pt(1)–P(3)	84.9(3)	85.8(3)
C(1)–Pt(1)–Tl(1)	92.7(3)	C(2)–Pt(1)–P(3)	168.7(3)	1675(3)
C(2)–Pt(1)–Tl(1)	89.5(3)	P(1)–Pt(1)–P(3)	99.3(1)	99.19(8)
P(3)–Pt(1)–Tl(1)	89.23(6)	C(1)–Pt(1)–Cu(1)	95.9(3)	97.5(3)
P(1)–Pt(1)–Tl(1)	95.61(6)	C(2)–Pt(1)–Cu(1)	105.5(3)	104.9(3)
C(4)–Pt(2)–C(3)	83.2(4)	P(1)–Pt(1)–Cu(1)	83.87(7)	83.24(6)
C(4)–Pt(2)–P(2)	91.9(3)	P(3)–Pt(1)–Cu(1)	77.16(7)	77.40(6)
C(3)–Pt(2)–P(2)	174.7(3)	C(3)–Pt(2)–C(4)	82.6(4)	82.1(4)
C(4)–Pt(2)–P(4)	168.4(2)	C(3)–Pt(2)–P(4)	91.8(3)	91.3(3)
C(3)–Pt(2)–P(4)	86.0(3)	C(4)–Pt(2)–P(4)	174.4(3)	173.4(3)
P(2)–Pt(2)–P(4)	99.06(9)	C(3)–Pt(2)–P(2)	168.4(3)	168.7(3)
C(4)–Pt(2)–Tl(1)	88.0(2)	C(4)–Pt(2)–P(2)	86.7(3)	87.4(3)
C(3)–Pt(2)–Tl(1)	91.2(3)	P(4)–Pt(2)–P(2)	98.92(9)	99.17(8)
P(2)–Pt(2)–Tl(1)	86.63(6)	C(3)–Pt(2)–Cu(1)	102.9(3)	102.5(3)
P(4)–Pt(2)–Tl(1)	96.46(6)	C(4)–Pt(2)–Cu(1)	98.9(3)	98.1(3)
Pt(1)–Tl(1)–Pt(2)	157.88(2)	P(4)–Pt(2)–Cu(1)	83.10(7)	83.24(6)
		P(2)–Pt(2)–Cu(1)	74.34(7)	74.92(6)
		N(1)–Cu(1)–N(2)	140.1(3)	138.8(3)
		N(1)–Cu(1)–Pt(1)	100.7(2)	101.6(2)
		N(2)–Cu(1)–Pt(1)	96.5(2)	96.4(2)
		N(1)–Cu(1)–Pt(2)	95.4(2)	94.6(2)
		N(2)–Cu(1)–Pt(2)	99.0(2)	98.8(2)
		Pt(1)–Cu(1)–Pt(2)	132.67(5)	134.27(5)

NP_2Pt . The $^{31}\text{P}\{^1\text{H}\}$ NMR spectrum of **1** shows a singlet at δ 29.1 ppm with $^1J(^{195}\text{Pt}, ^{31}\text{P}) = 1883$ Hz. The singlet indicates that all phosphorus atoms coordinated to the platinum atoms are equivalent, and the value of the coupling constant indicates that each phosphorus atom is trans to a methyl group.¹³ Considering the rigidity of the ligand and the occurrence of its dimeric complexes $\text{Pt}_2\text{X}_4(\mu\text{-L})_2$ as both cis ($\text{X} = \text{Cl}$) and trans ($\text{X} = \text{I}$) isomers,^{7c} we presumed that complex **1** could be formulated as *cis*- $\text{Pt}_2\text{Me}_4(\mu\text{-L})_2$. When this binuclear complex was reacted with TlClO_4 in CH_2Cl_2 in molar ratio 1:1, the yellow product [*cis*- $\text{Me}_3\text{Pt}_2\text{Tl}(\mu\text{-L})_2$] ClO_4 (**2**) was isolated in 60% yield (Scheme 1). The $^{31}\text{P}\{^1\text{H}\}$ NMR spectrum of **2** shows a singlet at δ 32.7 ppm with $^1J(^{195}\text{Pt}, ^{31}\text{P}) = 1688$ Hz, which is similar to those of platinum complexes in which the phosphine ligand is trans to a methyl group.¹³ No coupling of ^{31}P to Tl was observed for complex **2**, which is consistent with the finding in Catalano's work.^{4a} Complex **2** was reacted with $[\text{Cu}(\text{MeCN})_4]\text{ClO}_4$ in molar ratio 1:1 to afford red-orange compound **3**, [*cis*- $\text{Me}_4\text{Pt}_2\text{Cu}(\mu\text{-L})_2$] ClO_4 , in almost quantitative yield. An analogous reaction of **1** with $[\text{Cu}(\text{MeCN})_4]\text{BF}_4$ afforded compound **4**, [*cis*- $\text{Me}_4\text{Pt}_2\text{Cu}(\mu\text{-L})_2$] BF_4 , in 80% yield. The $^{31}\text{P}\{^1\text{H}\}$ NMR spectra of **3** and **4** at room temperature each

(13) Nixon, J. F.; Pidcock, A. *Annu. Rev. NMR Spectrosc.* **1969**, *2*, 345.
 (b) Pidcock, A.; Richarde, R. E.; Venanzi, L. M. *Proc. Chem. Soc.* **1962**, 184.

Scheme 1


consist of a singlet at δ 33.9 ppm with $^1J(^{195}\text{Pt}, ^{31}\text{P}) = 1586$ Hz, which is similar to those of platinum complexes in which the phosphine ligand is trans to a methyl group.¹³

ORTEP drawings with atom numbering for the cations of **2** and **3** are shown in Figures 2 and 3, respectively. The crystals of **3**·0.5H₂O and **4**·0.5H₂O constitute an isomorphous pair. The selected bond distances and angles of compounds **2**–**4** are given in Table 2. The L ligands in these complexes all adopt coordination mode D. The pair of cis-coordinated phosphorus atoms belonging to different L ligands are coplanar with the methyl groups and the platinum atom. The planarity of the coordination geometry around each platinum atom was assessed by fitting a least-squares plane to it and the coordinated phosphorus and carbon atoms, and the dihedral angles between the PtP_2 and PtC_2 fragments were also calculated (Table 3). The P–Pt–P bond angles are larger than the Me–Pt–Me angles. In the cation of compound **2**, the Pt–Tl bond lengths are 2.7961(7) and 2.8090(1) Å, which are comparable to the sum of the metallic radii of Pt and Tl (2.78 Å) and the measured values 2.994 Å in $\text{Ph}_3\text{PPt}(\text{C}_6\text{F}_5)_2\text{-TlMeCO}_2$, 2.884 Å in $(n\text{-Bu}_4\text{N})_2[\text{Pt}(\text{C}_6\text{F}_5)_3\text{TlMe}_2\text{CO}_2]_2$,^{4c} 3.135 Å in $\text{Pt}(\text{C}_6\text{F}_5)_2(\text{t-Bu-C}\equiv\text{C-})_2\text{TlMe}_2\text{CO}$,^{4d} 2.698 and 2.708 Å in $(\text{Bu}_4\text{N})_2\text{Pt}_2(\text{C}_6\text{F}_5)_8\text{Tl}$,^{4e} and 2.8888(5) Å in $\text{Pt}(\text{Ph}_2\text{Py})_3\text{TlNO}_3$,^{4f} indicating that the metal–metal interaction is genuinely attractive. The distances of the thallium atom with the two pyridyl nitrogen atoms are 2.824 and 2.844 Å, which are much longer than those in pyridine–thallium(I) complexes and the sum of the van der Waals radii of thallium and nitrogen atoms, indicating that the pyridyl lone pairs do not have the proper directionality for covalent interaction with the thallium atom. Furthermore, the Pt–Tl–Pt angle is 157.88(2)° with the Tl atom bending away from the two nitrogen atoms, so the thallium ion in **2** is encapsulated mainly by platinum–thallium binding. This is different from the case in $[\text{TlRh}_4(\mu\text{-pyS}_2)_2(\text{cod})_4]$,¹⁴ in which the Tl^+ ion is involved in both Rh–Tl and Tl–N interactions. The reason seems to be attributable to the fact that the Pt–Tl bonding interaction is stronger than the Rh–Tl bonding interaction. In the cation of compounds **3** and **4**, the copper atom displays a slightly distorted tetrahedral coordination geometry. The Pt–Cu bonds are about 2.6 Å in length, which is smaller

(14) Casado, M. A.; Pérez-Torrente, J. J.; López, J. A.; Ciriano, M. A.; Lahoz, F. J.; Oro, L. A. *Inorg. Chem.* **1999**, *38*, 2482.

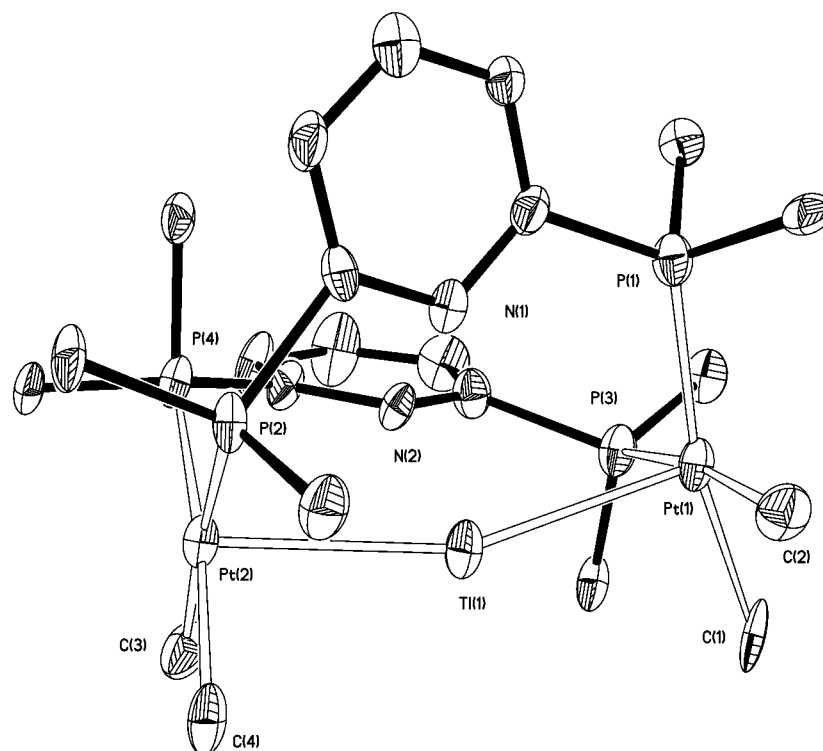


Figure 2. Perspective drawing (35% thermal ellipsoids) of the trinuclear cation $[cis\text{-Me}_4\text{Pt}_2\text{Ti}(\mu\text{-L})_2]^+$ in compound **2** with atomic numbering. For each phenyl ring in a Ph_2P group, only the *ipso* carbon atom is shown.

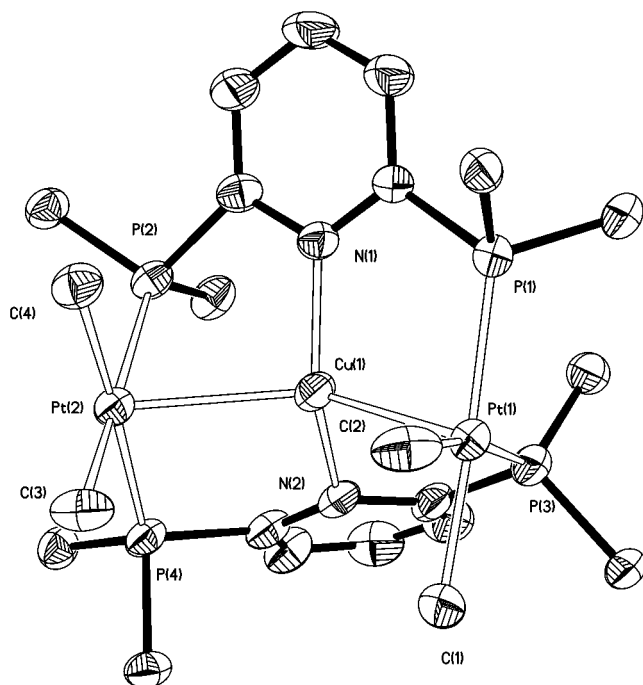


Figure 3. Perspective drawing (35% thermal ellipsoids) of the trinuclear cation $[cis\text{-Me}_4\text{Pt}_2\text{Cu}(\mu\text{-L})_2]^+$ in compound **3** with atomic numbering. For each phenyl ring in a Ph_2P group, only the *ipso* carbon atom is shown. The same atom numbering system is used for compound **4**.

than the sum of metallic radii of platinum and copper and similar to those of 2.577–2.888 Å in platinum carbonyl clusters.¹⁵ The Cu–N bonds are about 1.96 Å, which is a normal pyridine–copper distance. The angles of Pt–Cu–Pt are 132.67(5)° and 134.27(5)°. Judging from the Cu–Pt and Cu–N bond lengths, the copper(I) ion is encapsulated

Table 3. Deviation from a Least-squares Plane and Dihedral Angles of the Plane PtP_2 and PtC_2 in Compound **2–4**

	2	3	4
deviation from a least-squares plane (PtC ₂ P ₂) (Å)	Pt(1) 0.08 Pt(2) 0.05	Pt(1) 0.02 Pt(2) 0.04	Pt(1) 0.01 Pt(2) 0.04
dihedral angles of the plane PtP ₂ and PtC ₂ (°)	Pt(1) 8.4 Pt(2) 4.4	Pt(1) 1.9 Pt(2) 4.4	Pt(1) 0.8 Pt(2) 4.1

by both ligand–metal and platinum–copper interactions. This means that the metallomacrocyclic complex **1** has a stronger coordination affinity for Cu^+ than Tl^+ . It also accounts for the observation that the Tl^+ ion in compound **2** can be readily displaced by Cu^+ .

When compound **1** was reacted with AgBF_4 in MeCN in molar ratio 1:1, the expected product $[cis\text{-Me}_4\text{Pt}_2\text{Ag}(\mu\text{-L})_2]\text{-BF}_4$ was not obtained, but instead, $[\text{Me}_2\text{Pt}(\mu\text{-L})_2\text{Ag}_2(\text{MeCN})_2]\text{-}(\text{BF}_4)_2 \cdot \text{MeCN}$, **5**·MeCN, was isolated in 38% yield (Scheme 2). This finding differed from that in a similar reaction with a thallium(I) or copper(I) salt and can be rationalized on the grounds that argentophilicity is stronger than cuprophilicity.^{6d} Compound **5** can also be obtained from the reaction of $[\text{Ag}_2(\text{MeCN})_2(\mu\text{-L})_n(\text{BF}_4)_{2n}]$ with $\text{Me}_2\text{Pt}(\text{cod})$ in almost quantitative yield (Scheme 2). The $^{31}\text{P}\{^1\text{H}\}$ NMR spectrum of **5** at room temperature consists of a singlet at δ 34.8 ppm with $^1J(^{195}\text{Pt}, ^{31}\text{P}) = 1547$ Hz, which is similar to those of platinum phosphine complexes, and a doublet of doublets at δ 25.1 ppm with $^1J(^{109}\text{Ag}, ^{31}\text{P}) = 529$ Hz and $^1J(^{107}\text{Ag}, ^{31}\text{P}) = 457$ Hz. These values are comparable to those in $\text{Ag}(\text{PCy}_3)_2(\text{NO}_3)$ ($\delta = 32.8$ ppm, $^1J(^{109}\text{Ag}, ^{31}\text{P}) = 527$ Hz and $^1J(^{107}\text{Ag}, ^{31}\text{P})$

(15) Liu, H.; Tan, A. L.; Mok, K. F.; Mak, T. C. W.; Batsanov, A. S.; Howard, J. A. K.; Hor, T. S. A. *J. Am. Chem. Soc.* **1997**, *119*, 11006. (b) Braunstein, P.; Freyburger, S. *J. Organomet. Chem.* **1988**, *352*, C29.

Table 4. Selected Bond Distances (Å) and Angles (deg) for Complexes **5** and **6**

5		6	
Pt(1)–C(1)	2.096(7)	Fe(1)–C(1)	1.800(5)
Pt(1)–C(2)	2.113(7)	Fe(1)–C(2)	1.769(4)
Pt(1)–P(1)	2.301(2)	Fe(1)–C(3)	1.787(4)
Pt(1)–P(3)	2.300(2)	Fe(1)–P(1)	2.224(1)
Pt(1)–Ag(1)	2.8190(7)	Fe(1)–P(1A)	2.229(1)
Ag(1)–N(3)	2.244(8)	Fe(1)–Ag(1)	2.7135(6)
Ag(1)–N(2)	2.377(6)	Ag(1)–N(1)	2.402(3)
Ag(1)–N(1)	2.476(6)	Ag(1)–N(1A)	2.460(3)
Ag(1)–Ag(2)	2.9061(9)	Ag(1)–C(1)	2.632(4)
Ag(2)–N(4)	2.38(2)	Ag(1)–Ag(2)	2.9267(5)
Ag(2)–P(4)	2.403(2)	Ag(2)–P(2A)	2.418(1)
Ag(2)–P(2)	2.408(2)	Ag(2)–P(2)	2.421(1)
Ag(2)–N(4')	2.43(3)	Ag(2)–O(4)	2.456(3)
C(1)–Pt(1)–C(2)	82.3(3)	C(1)–Fe(1)–C(2)	108.4(2)
C(1)–Pt(1)–P(3)	169.5(2)	C(1)–Fe(1)–C(3)	139.3(2)
C(2)–Pt(1)–P(3)	87.2(2)	C(2)–Fe(1)–C(3)	112.3(2)
C(1)–Pt(1)–P(1)	90.6(2)	C(2)–Fe(1)–P(1)	89.7(1)
C(2)–Pt(1)–P(1)	172.9(2)	C(3)–Fe(1)–P(1)	90.2(1)
P(3)–Pt(1)–P(1)	99.88(6)	C(1)–Fe(1)–P(1)	89.5(1)
C(1)–Pt(1)–Ag(1)	99.3(3)	C(2)–Fe(1)–P(1A)	91.1(1)
C(2)–Pt(1)–Ag(1)	96.0(2)	C(3)–Fe(1)–P(1A)	90.8(1)
P(3)–Pt(1)–Ag(1)	82.77(5)	C(1)–Fe(1)–P(1A)	88.9(1)
P(1)–Pt(1)–Ag(1)	85.15(5)	P(1)–Fe(1)–P(1A)	178.35(4)
N(3)–Ag(1)–N(2)	134.0(3)	C(2)–Fe(1)–Ag(1)	175.9(1)
N(3)–Ag(1)–N(1)	104.9(3)	C(3)–Fe(1)–Ag(1)	71.4(1)
N(2)–Ag(1)–N(1)	120.7(2)	C(1)–Fe(1)–Ag(1)	67.9(1)
N(3)–Ag(1)–Pt(1)	102.3(2)	P(1)–Fe(1)–Ag(1)	88.50(3)
N(2)–Ag(1)–Pt(1)	84.5(2)	P(1A)–Fe(1)–Ag(1)	90.60(3)
N(1)–Ag(1)–Pt(1)	89.8(1)	N(1)–Ag(1)–N(1A)	161.4(1)
N(3)–Ag(1)–Ag(2)	87.1(2)	N(1)–Ag(1)–C(1)	102.0(1)
N(2)–Ag(1)–Ag(2)	85.8(2)	N(1A)–Ag(1)–C(1)	88.6(1)
N(1)–Ag(1)–Ag(2)	92.1(1)	N(1)–Ag(1)–Fe(1)	89.87(7)
Pt(1)–Ag(1)–Ag(2)	169.63(3)	N(1A)–Ag(1)–Fe(1)	88.81(7)
N(4)–Ag(2)–P(4)	101.9(4)	C(1)–Ag(1)–Fe(1)	39.3(1)
N(4)–Ag(2)–P(2)	101.1(4)	N(1)–Ag(1)–Ag(2)	91.21(7)
P(4)–Ag(2)–P(2)	156.15(8)	N(1A)–Ag(1)–Ag(2)	90.18(7)
N(4)–Ag(2)–N(4')	29.5(6)	C(1)–Ag(1)–Ag(2)	140.3(1)
P(4)–Ag(2)–N(4')	108.1(6)	Fe(1)–Ag(1)–Ag(2)	178.92(2)
P(2)–Ag(2)–N(4')	95.1(6)	P(2A)–Ag(2)–P(2)	148.52(4)
N(4)–Ag(2)–Ag(1)	176.0(5)	P(2A)–Ag(2)–O(4)	98.6(1)
P(4)–Ag(2)–Ag(1)	76.10(5)	P(2)–Ag(2)–O(4)	106.0(1)
P(2)–Ag(2)–Ag(1)	80.60(6)	P(2A)–Ag(2)–Ag(1)	79.26(3)
N(4')–Ag(2)–Ag(1)	154.3(6)	P(2)–Ag(2)–Ag(1)	78.02(2)
		O(4)–Ag(2)–Ag(1)	173.9(1)

= 455 Hz), Ag(PCy₃)₂(ClO₄) (δ = 37.3 ppm, $^1J(^{109}\text{Ag}, ^{31}\text{P})$ = 534 Hz and $^1J(^{107}\text{Ag}, ^{31}\text{P})$ = 462 Hz), and Ag₂(NO₃)₂(m-PP)₂ (m-PP = 1,3-bis(diphenylphosphino)methylbenzene, δ = 5.0 ppm, $^1J(^{109}\text{Ag}, ^{31}\text{P})$ = 525 Hz and $^1J(^{107}\text{Ag}, ^{31}\text{P})$ = 457 Hz).¹⁶ Compared to the singlets at ambient temperature in [Ag₂(MeCN)₂(μ -L)]_nⁿ⁺ and [Ag₂(μ -L)₃]₂²⁺ that are indicative of the rapid phosphine ligand exchange equilibria,^{7h,i} the existence of a pair of doublets in **5** due to coupling of ³¹P to both ¹⁰⁷Ag and ¹⁰⁹Ag indicates that the phosphorus ligand exchange rates are drastically decreased, and the metal core is rather stable in solution at ambient temperature.

An ORTEP drawing with atom numbering for the [cis-Me₂PtAg₂(μ -L)₂(MeCN)₂]²⁺ dication of **5** is shown in Figure 4. The platinum atom has square-planar geometry, the methyl groups being coplanar with the pair of cis-coordinated phosphorus atoms belonging to different L ligands (P(1)–

Pt(1)–P(3) angle = 99.88(6)°). The middle silver atom of the linear Pt(II)–Ag(I)–Ag(I) chain lies perpendicular to the P₂PtMe₂ plane with a Pt–Ag distance of 2.8190(7) Å, which is slightly shorter than the sum of their metallic radii (2.83 Å), suggesting the existence of strong Pt(II)→Ag(I) dative bonding. This distance lies within the range 2.6–3.0 Å for known complexes containing a Pt→Ag dative bond.¹⁷ On the other hand, the distance between the silver atoms is 2.9061(9) Å, which is similar to those (2.934(2), 2.946(2) Å) in [Ag₂(H₂L)₃]_n²ⁿ⁺ (H₂L = N',N'-bis(salicylidene)-1,4-di-aminobutane),^{18a} (2.936(1)–2.960(1) Å) in [Ag₂(μ -dcpm)₂]⁺ (dcpm = bis(dicyclohexylphosphino)methane),^{18b} (2.7–3.0 Å) in polyhedral silver cages each encapsulating a C₂²⁻ anion (C₂@Ag_n, n = 6–9),^{18d} and (2.953(2)–2.986(2) Å) in silver-alkynyl cage compounds [Ag₁₄(μ -C≡C–tBu)₁₂X]Y (X = Cl, Br; Y = OH, BF₄).^{18e} These distances are suggestive of significant argentophilic interaction between the silver(I) centers.¹⁸ The Pt(II)–Ag(I)–Ag(I) chain deviates significantly from linearity with Pt(1)–Ag(1)–Ag(2) = 169.63(3)°. The coordination environment about the Ag(1) atom can be described as a trigonal bipyramid with Pt(1) and Ag(2) occupying axial positions and two pyridyl rings and the MeCN ligand lying in the equatorial plane, the sum of the three N–Ag–N angles being almost 360°. The terminal MeCN ligand attached to Ag(2) exhibits 2-fold disorder.

The attractive metal–metal interactions in **2–5** can be rationalized by employing a qualitative MO diagram proposed by Balch et al.^{3b} for trinuclear systems of electronic configuration d⁸d¹⁰d⁸ for Ir^IAu^IIr^I, d¹⁰d⁸d¹⁰ for Au^IIr^IAu^I, and d⁸s²d⁸ for Ir^ITl^IIr^I by combining the filled d_{z²} and empty p_z orbitals on the transition metals with the filled Tl 6s and empty Tl 6p_z orbitals for **2**, and combining the filled d_{z²} and empty p_z orbitals on the transition metals for **3–5**. Mixing between levels stabilizes the filled orbitals relative to their unfilled counterparts, leading to an attractive interaction between metal centers.

In complexes **1–5**, the pair of L ligands coordinated with the metal atom is arranged in cis positions. To achieve a trans arrangement of L ligands in a trinuclear complex, we chose an iron carbonyl group to replace the platinum atom. The reaction of 1 equiv of H₂Fe(CO)₄ (prepared from K[HF₂(CO)₄]) with 2.5 equiv of ligand L in EtOH/CH₂Cl₂ under acidic conditions yielded *trans*-Fe(CO)₃(L)₂, in which only one phosphorus atom of L is coordinated to the iron atom. Its IR ν (CO) spectrum exhibits a strong peak at 1881 cm⁻¹ and a weak peak at 1974 cm⁻¹ which are similar to those of *trans*-Fe(CO)₃(R₃P)₂.¹⁹ Using *trans*-Fe(CO)₃(L)₂ to react with

(16) Caruso, F.; Camalli, M.; Rimml, H.; Venanzi, L. M. *Inorg. Chem.* **1995**, *34*, 673 and references therein. (b) Bowmaker, G. A.; Effendy, Harvey, P. J.; Healy, P. C.; Skelton, B. W.; White, A. H. *J. Chem. Soc., Dalton Trans.* **1996**, 2449 and references therein. (c) Catalano, V. J.; Kar, H. M.; Garnas, J. *Angew. Chem., Int. Ed.* **1999**, *38*, 1979.

(17) Fornié, J.; Martin, A. In *Metal Clusters in Chemistry*; Braunstein, P., Ora, L. A., Raithby, P. R., Eds.; Wiley-VCH, Weinheim, 1999, vol. 1, pp 417–443. (b) Yamaguchi, T.; Yamazaki, F.; Ito, T. *J. Am. Chem. Soc.* **2001**, *123*, 743.

(18) Tong, M.-L.; Chen, X.-M.; Ye, B.-H.; Ji, L.-N. *Angew. Chem., Int. Ed.* **1999**, *38*, 2237. (b) Che, C.-M.; Tse, M.-C.; Chan, M. C. W.; Cheung, K.-K.; Phillips, D. L.; Leung, K. H. *J. Am. Chem. Soc.* **2000**, *122*, 2464. (c) Rawashdeh-Omary, M. A.; Omary, M. A.; Patterson, H. H. *J. Am. Chem. Soc.* **2000**, *122*, 10371. (d) Wang, Q.-M.; Mak, T. C. W. *Chem. Commun.* **2001**, 807 and references therein. (e) Rais, D.; Yau, J.; Mingos, D. M. P.; Vilar, R.; White, A. J. P.; Williams, D. J. *Angew. Chem., Int. Ed.* **2001**, *40*, 3464.

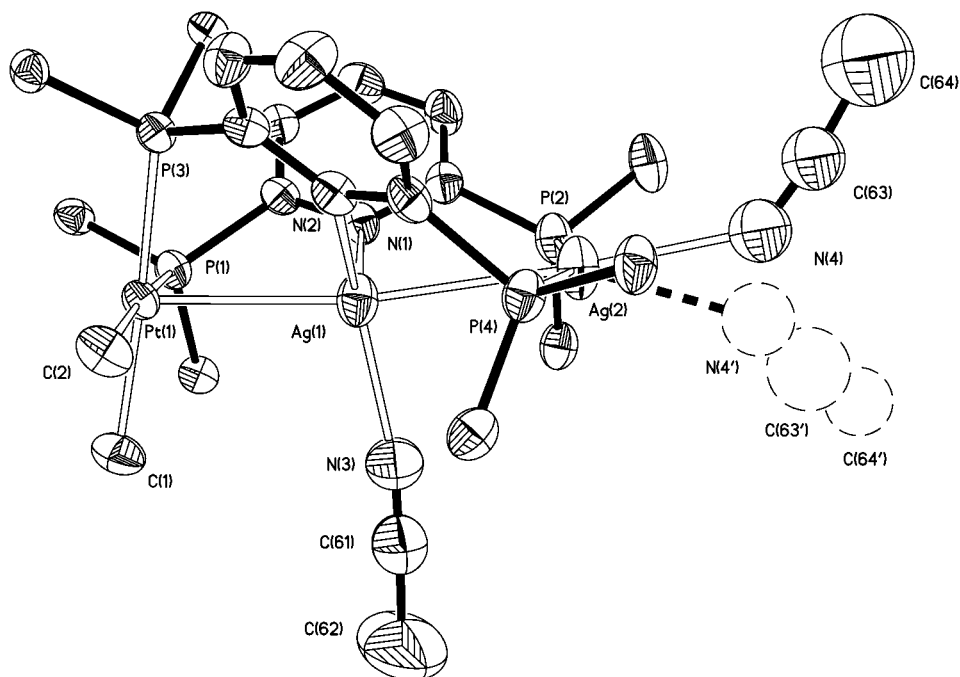
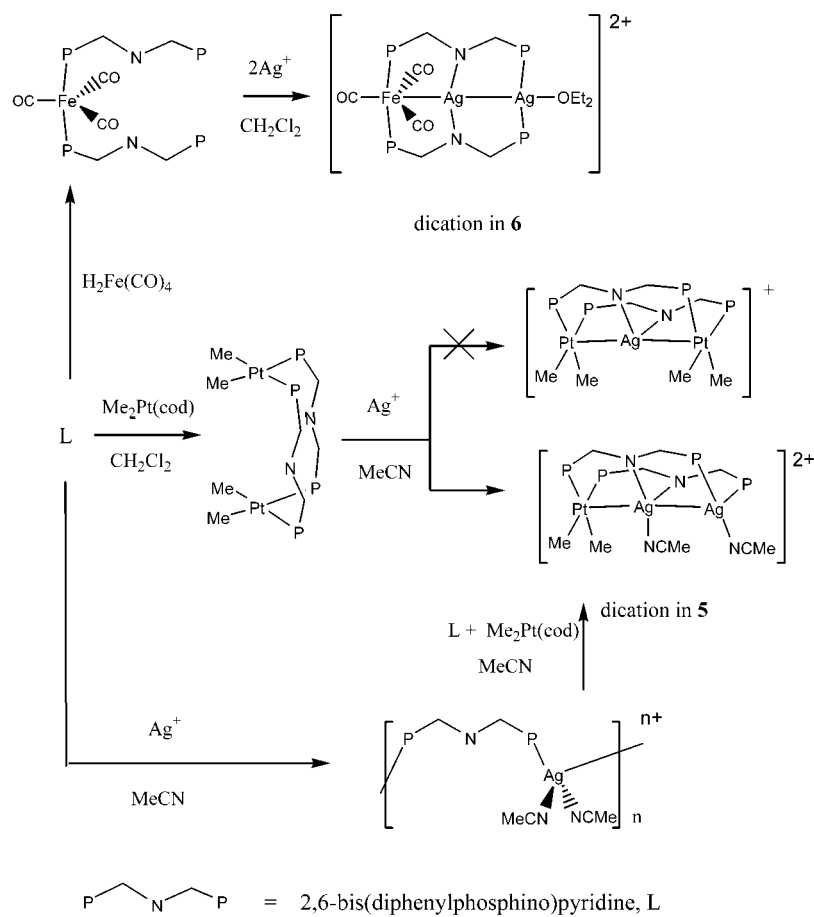


Figure 4. Perspective drawing (35% thermal ellipsoids) of the trinuclear cation $[cis-Me_2PtAg_2(\mu-L)_2(MeCN)_2]^{2+}$ in compound **5** with atomic numbering. For each phenyl ring in a Ph_2P group, only the ipso carbon atom is shown. The MeCN ligand bonded to Ag(2) exhibits 2-fold disorder and is shown in two equally populated orientations.

Scheme 2



2 equiv of $AgClO_4$ in CH_2Cl_2 , the trinuclear compound $[(CO)_3Fe(\mu-L)_2Ag_2(Et_2O)](ClO_4)_2$ (**6**) was precipitated by Et_2O in 65% yield (Scheme 2). The IR $\nu(CO)$ spectrum of

6 exhibits three peaks that are shifted to higher frequencies (1991s, 1931s, and 1896s), which are similar to those of binuclear complexes containing an $Fe^0 \rightarrow M^{n+}$ bond.^{7n,19} The

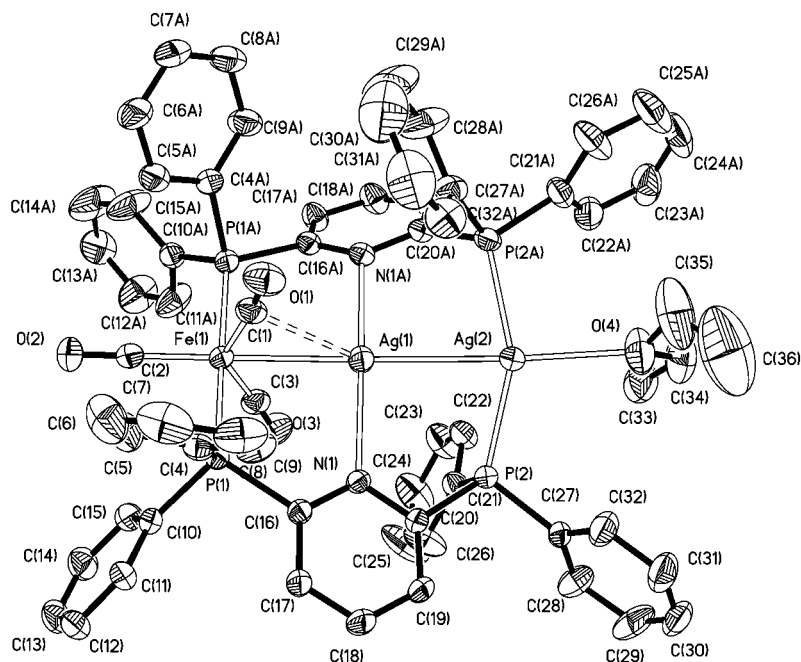


Figure 5. Perspective drawing (35% thermal ellipsoids) of the trinuclear cation $[trans\text{-Fe}(\text{CO})_3\text{Ag}_2(\mu\text{-L})_2(\text{Et}_2\text{O})]^{2+}$ in compound **6** with atomic numbering scheme.

$^{31}\text{P}\{^1\text{H}\}$ NMR spectrum of **6** at room temperature consists of a doublet at δ 87.2 ppm with $J(\text{Ag}, \text{P}) = 12$ Hz for the response of phosphorus atoms bonded to iron, which is attributed to the sum of coupling via the Fe atom and via the pyridine group. This coupling value is the same as that of the $\text{Fe}(0) \rightarrow \text{Ag}(\text{I})$ dative bond in $[\{\text{Fe}(\text{CO})_4\}_2\text{Ag}(\mu\text{-L})]\text{ClO}_4$ ($J(\text{Ag}, \text{P}) = 12$ Hz).⁷ⁿ On the other hand, the phosphorus atoms coordinated to silver generate a doublet of doublets at δ 27.8 ppm with $^1J(^{109}\text{Ag}, ^{31}\text{P}) = 536$ Hz and $^1J(^{107}\text{Ag}, ^{31}\text{P}) = 463$ Hz, which are similar to those of compound **6**. The coupling of ^{31}P and $^{107,109}\text{Ag}$ also suggests that coordination of L to the metal core effectively stops the phosphorus ligand exchange.

An ORTEP drawing with atom numbering for the $[trans\text{-Fe}(\text{CO})_3\text{Ag}_2(\mu\text{-L})_2(\text{Et}_2\text{O})]^{2+}$ dication of **6** is shown in Figure 5. The complex features a linear $\text{Fe}(\text{I})-\text{Ag}(\text{I})-\text{Ag}(\text{I})$ chain in which there is bonding interaction between adjacent metal atoms. The complex displays a distorted octahedral geometry at the iron atom, in which the FeP_2 unit is nearly linear with a $\text{P}(1)-\text{Fe}(1)-\text{P}(1\text{A})$ angle of $178.35(4)^\circ$, with three CO moieties and atom $\text{Ag}(1)$ lying in a plane perpendicular to the FeP_2 axis. The $\text{Fe}-\text{Ag}$ bond distance of $2.7135(6)$ Å is comparable to those in complexes containing neutral iron carbonyl groups, as in $[\text{Fe}(\text{CO})_3(\mu\text{-Ph}_2\text{Ppy})_2\text{Ag}(\text{Ph}_2\text{Ppy})]\text{ClO}_4$ ^{19a} ($2.760(1)$ Å) and $[\{\text{Fe}(\text{CO})_4\}_2\text{Ag}(\mu\text{-L})]\text{ClO}_4$ ($2.627(3)$ and $2.652(3)$ Å),⁷ⁿ as well as those in iron-silver clusters containing Collman's reagent $\text{Fe}(\text{CO})_4^{2-}$, as in $[\text{Fe}_8(\text{CO})_{32}\text{Ag}_{13}]^{4-}$ ($2.695\text{--}2.762$ Å), $[\text{Fe}_4(\text{CO})_{16}\text{Ag}_4]^{4-}$ ($2.570\text{--}2.600$ Å), $[\text{Fe}_4(\text{CO})_{16}\text{Ag}_5]^{3-}$ ($2.585\text{--}2.727$ Å), $\text{Fe}_4(\text{CO})_{16}\text{Ag}_8(\text{dppm})_2$ ($2.608\text{--}2.666$ Å), and $\text{Fe}_4(\text{CO})_{16}\text{Ag}_4\text{Au}_4(\text{dppe})_2$ ($2.643\text{--}2.711$ Å).²⁰ There is also a weak interaction between the

$(\text{CO})_1$ ligand and the middle silver atom ($\text{Ag}(1)-\text{C}(1) = 2.632(2)$ Å), which is coordinated by two pyridyl rings at slightly longer distances ($2.402(3)$ and $2.460(3)$ Å) than those of pyridine-silver complexes in the range $\text{Ag}-\text{N} = 2.10\text{--}2.36$ Å.²¹ The longer observed $\text{Ag}-\text{N}$ distance may be attributed to inefficient coordination of the pyridine lone pair to the silver atom as the $\text{C}18(\text{A})\cdots\text{N}1(\text{A})-\text{Ag}1$ angle of 149.1° is far from the ideal value of 180° . The distance between the silver atoms is $2.9267(5)$ Å, which is in agreement with those in **1** and other complexes displaying argentophilicity. The $\text{Ag}(2)$ atom is coordinated by two phosphorus atoms and an ether oxygen atom with $\text{Ag}(2)-\text{P}(2) = 2.421(1)$ Å, $\text{Ag}(2)-\text{P}(2\text{A}) = 2.418(1)$ Å, and $\text{Ag}(2)-\text{O}(4) = 2.456(3)$ Å. The ether oxygen atom and the three metals are almost collinear with $\text{Fe}(1)-\text{Ag}(1)-\text{Ag}(2) = 178.92(2)^\circ$ and $\text{Ag}(1)-\text{Ag}(2)-\text{O}(4) = 173.9(1)^\circ$.

Recently, the importance of argentophilicity in coordination and cluster chemistry has been well recognized.¹⁸ According to spectroscopic evidence and extended Hückel calculations, the $\text{Ag}(\text{I})-\text{Ag}(\text{I})$ bond energy in the ground state is 25 kJ/mol,²² comparable to the $\text{Au}(\text{I})-\text{Au}(\text{I})$ bond energy (32 kJ/mol)²² and strong hydrogen bond energy (up to 45 kJ/mol)²³ which have been exploited in cluster synthesis and

(19) Li, S.-L.; Mak, T. C. W.; Zhang, Z.-Z. *J. Chem. Soc., Dalton Trans.* **1996**, 3475. (b) Song, H.-B.; Wang, Q.-M.; Zhang, Z.-Z.; Mak, T. C. W. *J. Organomet. Chem.* **2000**, 605, 15.

(20) Albano, V. G.; Grossi, L.; Longoni, G.; Monari, M.; Mulley, S.; Sironi, A. *J. Am. Chem. Soc.* **1992**, 114, 5708. (b) Albano, V. G.; Azzaroni, F.; Iapalucci, M. C.; Longoni, G.; Monari, M.; Mulley, S.; Proserpio, D. M.; Sironi, A. *Inorg. Chem.* **1994**, 33, 5320. (c) Albano, V. G.; Iapalucci, M. C.; Longoni, G.; Monari, M.; Paselli, A.; Zacchini, S. *Organometallics* **1998**, 17, 4438.

(21) Baum, G.; Constable, E. C.; Fenske, D.; Housecroft, C. E.; Kulke, T. *Chem. Commun.* **1998**, 2659. (b) Kaes, C.; Hosseini, M. W.; Rickard, C. E. F.; Skelton, B. W.; White, A. H. *Angew. Chem., Int. Ed.* **1998**, 37, 920. (c) Carlucci, L.; Ciani, G.; Proserpio, D. M. *Chem. Commun.* **1999**, 449.

(22) Rawashdeh-Omary, M. A.; Omary, M. A.; Patterson, H. H.; Fackler, J. P., Jr. *J. Am. Chem. Soc.* **2001**, 123, 11237.

(23) Jeffery, G. A. *An Introduction to Hydrogen Bonding*; Oxford University Press: Oxford, U.K., 1997.

crystal engineering. Complexes **5** and **6** are the first linear heterotrinnuclear systems featuring coordination mode E for the bridging ligand L, with the argentophilic interaction playing a dominant role in stabilizing the trinuclear dication in solution.

Electronic Absorption and Emission Spectra of 1–5. The electronic spectra of complexes **1–5** in CH₂Cl₂ exhibit absorption peaks at about 240 nm that are tentatively assigned to intraligand transition. The low energy band of thallium complex **2** occurs at about 390 nm ($\epsilon_{\max} = 1.4 \times 10^4 \text{ dm}^3 \text{ mol}^{-1} \text{ cm}^{-1}$), and those of copper complexes **3** and **4** occur at 340 nm ($\epsilon_{\max} = 2.6 \times 10^4 \text{ dm}^3 \text{ mol}^{-1} \text{ cm}^{-1}$), which are tentatively assigned to the metal–metal bonded $d_{\sigma^*} \rightarrow p_{\sigma}$ transition. The electronic spectrum of **5** is similar to that of **1**.

Unlike the platinum systems studied by Catalano and co-workers,^{4a} upon excitation at 340 nm for **2–4** and 315 nm for **5**, the CH₂Cl₂ ($2 \times 10^{-5} \text{ dm}^3 \text{ mol}^{-1}$) solutions of complexes **2–5** at room temperature show photoemission at 598 nm with lifetime of 0.7 μs for **2**, 537 nm with lifetime of 3.7 μs for **3** and **4**, and 540 nm with lifetime of 2.1 μs for **5**. No photoluminescence was observed for **1** under the same condition. With reference to previous works,²⁴ we tentatively

assign the emission of **2–5** with λ_{\max} at 537–598 nm to transitions derived from excited electronic states of $^3[(d_{\sigma^*})(p_{\sigma})]$ origin.

Conclusion

We have utilized the bridging tridentate pyridino-phosphine ligand L to generate a twelve-membered alkyl platinum(II) metallomacrocyclic whose coordination ability to Tl⁺ and Cu⁺ is studied, plus two linear $d^8-d^{10}-d^{10}$ heterotrinnuclear systems that are stabilized by metal–metal (M→Ag(I), M = Fe(0), Pt(II)) dative bonding and argentophilic interaction.

Acknowledgment. This work is supported by Hong Kong Research Grants Council Earmarked Grants CUHK 4022/98P.

Supporting Information Available: X-ray crystallographic file in CIF format for compounds **2**·1.5THF, **3**·0.5H₂O, **4**·0.5H₂O, **5**·MeCN, and **6**. This material is available free of charge via the Internet at <http://pubs.acs.org>.

IC011293F

- (24) (a) Yip, H.-K.; Lin, H.-M.; Cheung, K.-K.; Che, C.-M.; Wang, Y. *Inorg. Chem.* **1994**, *33*, 1644. (b) Balch, A. L.; Nagle, J. K.; Oram, D. E.; Reedy, P. E., Jr. *J. Am. Chem. Soc.* **1988**, *110*, 454.